NASA
Technical
Paper
2473

July 1985

Hertzian Contact in Two and Three Dimensions

John H. Tripp

NASA

Hertzian Contact in Two and Three Dimensions

John H. Tripp

Lewis Research Center
Cleveland, Ohio

I

Summary

The basic solution to the problem of mechanical contact between elastically deforming solids was proposed by Hertz over a century ago and has been used by tribologists and others ever since in a steadily increasing number of applications. While the theoretical development is not conceptually difficult and treatments exist to suit all tastes, it is nonetheless interesting to trace the relationships among the solutions in different dimensions. Such an approach is used herein to shed light on the curious and sometimes perplexing behavior of line contacts. A final object of this brief review is simply to gather a number of the more frequently used contact expressions together as a convenient reference and for comparative purposes.

Introduction

In a recent review (ref. 1) Johnson first summarizes the fundamentals of contact mechanics as originally worked out by Hertz and then considers many of the subsequent developments and applications of the Hertz solution. For the great majority of cases, an application of Hertz theory requires little more than selecting the correct formula, and this end could be served by a simple handbook compilation. Subtleties do sometimes arise when using such expressions, however, particularly for line contacts where stresses and strains due to loading of a boundary element diminish at large distances only as fast as the inverse of the distance from that element. This implies that the material displacements themselves actually diverge logarithmically with distance, and if no boundaries intervene, the result may be hard to interpret. For such situations, an appreciation of the derivation of the expressions and the underlying assumptions becomes valuable.

Beginning with a fundamental solution to the problem of a point force on an elastic half-space, we first show how it is used to yield the solution for the problem of frictionless contact between the half-space and a rigid ellipsoidal punch. This fundamental point force solution is then transformed to the solution for a line force acting on the half-space, the equivalent of the point force problem in two dimensions. The problem of contact by a rigid circular punch, a cylinder in three dimensions, is

then solved in an analogous manner. From this, an approximate solution for a roller squeezed between parallel flats is derived and compared to the exact result. While the conventional Hertz analysis correctly yields the contact width for such configurations, its prediction for the compliance of nonplanar bodies is poor. This may be improved substantially by using elastic solutions specifically accounting for the geometry of the deforming body.

Finally, a comparative tabulation of the more useful formula in three and two dimensions is given. Since it is not one of our present aims, no exhaustive list of applications of Hertz theory is provided herein. Reference, however, may usefully be made to the bibliography compiled in reference 1.

Symbols

A_0	semiaxis of ellipsoid in x-direction, m
a	contact semiminor axis in three dimensions, m; contact semiwidth in two dimensions, m
a_0	semiminor axis of ellipsoid cross section in contact plane, m
B	complete elliptic integral
B_0	semiaxis of ellipsoid in y-direction, m
b	contact semimajor axis in three dimensions, m
b_0	semimajor axis of ellipsoid cross section in contact plane, m
C	bounding curve of contact region S
C_0	semiaxis of ellipsoid in z-direction, m
D	complete elliptic integral; diameter of body in z-direction, m
d	compliance, m
d_0	compliance datum, m
E	Young's modulus, Nm^{-2}
$\mathcal{E}$	complete elliptic integral of second kind
F	total load in three dimensions, N
J	general complete elliptic integral
K	complete elliptic integral of first kind
k	argument of complete elliptic integral
p	contact pressure in z-direction, Nm^{-2}

1

$\bar{p}$	mean contact pressure, Nm^{-2}
p_0	maximum (central) contact pressure, Nm^{-2}
q	total load per unit length in two dimensions, Nm^{-1}
R	radial polar coordinate, m; reciprocal of sum of principal curvatures of ellipsoid, $(R_x^{-1} + R_y^{-1})^{-1}$, m; radius of circular cylinder, m; reciprocal of sum of curvatures for two cylinders, $(R_1^{-1} + R_2^{-1})^{-1}$, m
R_0	radius of sphere, m
r	radial spherical coordinate, m; radial polar coordinate in S, m
S	surface of contact region
u,v,w	elastic displacement vector components, m
x,y,z	Cartesian coordinates, m
z	axial cylindrical coordinate, m
α	ratio of principal curvatures of ellipsoid, R_y/R_x
γ	Euler's constant
Γ	ratio of difference to sum of principal curvatures of ellipsoid
ϵ	eccentricity of contact ellipse
ζ	nondimensional z-coordinate, z/a
θ	azimuthal cylindrical coordinate
κ	ratio of major to minor axis of contact ellipse, b/a (ellipticity)
ν	Poisson's ratio
ξ	nondimensional x-coordinate, x/a
ρ	radial cylindrical coordinate, m
σ	normal stress, Nm^{-2}
τ	shear stress, Nm^{-2}
ϕ	azimuthal polar coordinate in S
ψ	azimuthal polar coordinate; digamma function

Fundamental Point Force Solution

Any convenient starting point may be adopted in deriving the stress tensor to solve a given elasticity problem. If the final result satisfies all the general and specific conditions of the problem, then the solution is acceptable. Thus, the stress tensor for the problem of a concentrated point force acting along the normal to the plane undeformed surface of an elastic half-space is chosen here as starting point, even though it too may be constructed from still more elementary results.

Since the force provides a symmetry axis for the basic problem, the coordinates most suited to its description

(a)

(b)
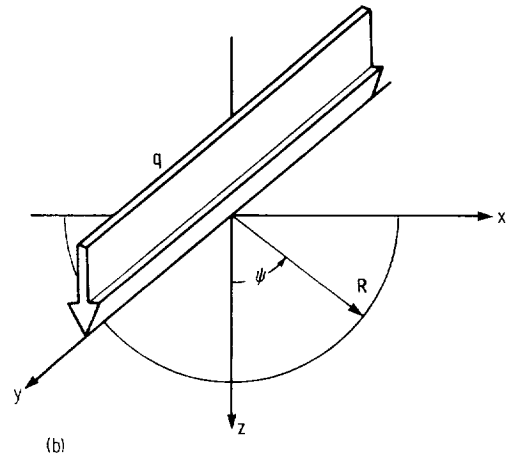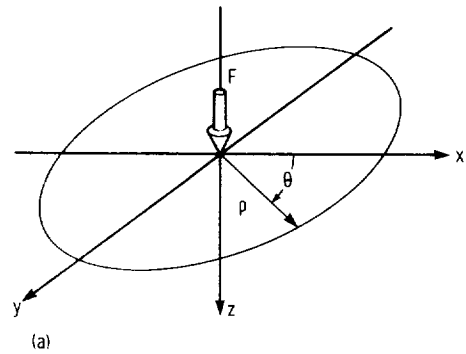
(a) Cylindrical polar coordinates used for a point force F acting in z-direction at the origin on the bounding surface of an elastic half-space.

(b) Plane polar coordinates used for a line force q acting in z-direction in $x=0$ plane on bounding surface of elastic half-space.

Figure 1.—Coordinate systems used in elasticity problems.

are the cylindrical system (ρ,θ,z) shown in figure 1(a). In reducing the dimensionality of the problem to discuss line contact parallel to the y-axis, a system of plane polar coordinates (R,ψ) in the x,z-plane is convenient, and these appear in figure 1(b). Once symmetry is violated, as in the ellipsoidal contact problem, the Cartesian system (x,y,z) provides a set of fixed directions for superimposing stresses arising from parallel but displaced point forces. It is straightforward to transform between the two polar systems by using the Cartesian system as intermediary.

Consider a point force F acting along the positive z-axis on the boundary surface $z=0$ of an elastic half-space defined by $z>0$ and having elastic constants E (Young's modulus) and ν (Poisson's ratio). By symmetry, polar angle θ does not appear in the stress tensor and components $\tau_{\rho\theta}$ and $\tau_{\theta z}$ vanish. The four remaining components are given by reference 2:

2

|

$$\sigma_\rho = \frac{F}{2\pi}\left[(1-2\nu)\left(\frac{1}{\rho^2} - \frac{z}{\rho^2 r}\right) - \frac{3z\rho^2}{r^5}\right]$$

$$\sigma_z = -\frac{3F}{2\pi}\frac{z^3}{r^5}$$

$$\sigma_\theta = \frac{F}{2\pi}(1-2\nu)\left(-\frac{1}{\rho^2} + \frac{z}{\rho^2 r} + \frac{z}{r^3}\right)$$

$$\tau_{\rho z} = -\frac{3F}{2\pi}\frac{\rho z^2}{r^5}$$

(1)

where

$$r = (x^2 + y^2 + z^2)^{1/2} = (\rho^2 + z^2)^{1/2}$$

is the spherical radial coordinate giving the distance from the point of application of the force. These stress components satisfy the general requirements of mechanical equilibrium and compatibility. They diminish to zero as the inverse square of r at large distance. On the plane boundary, components σ_z and $\tau_{\rho z}$ vanish except at the origin, and the net force acting over any hemispherical surface centered on the origin is readily shown to be F in the positive z-direction, independent of its radius. These are the special requirements of the singular solution (eq. (1)) which ensures that it describes the correct physical problem. The displacements in the directions of increasing (ρ, θ, z) compatible with equations (1) are found to be

$$u = \frac{(1-2\nu)(1+\nu)F}{2\pi E\rho}\left[\frac{z}{r} - 1 + \frac{1}{(1-2\nu)}\frac{\rho^2 z}{r^3}\right]$$

(2a)

$$v = 0$$

(2b)

$$w = \frac{F}{2\pi E}\left[\frac{(1+\nu)z^2}{r^3} + \frac{2(1-\nu^2)}{r}\right]$$

(2c)

Clearly, u and w are singular at the origin while the arbitrary reference value zero at infinity is approached as r^{-1}. To be physically acceptable, the singularities may be imagined to be excluded by replacing the point force with an appropriate distribution of stress over a finite surface enclosing a small volume around the origin. Strictly this distribution should be that given by equations (1), although, in practice, St. Venant's principle allows us to relax this requirement and to use any distribution which yields the same resultant force from the small excluded volume.

Contact In Three Dimensions

Rigid Ellipsoid and Elastic Half-Space

Clearly, the point force in equation (1) may be replaced by the force $p\,\delta S$ acting over a sufficiently small surface element δS due to any given distribution of normal pressure p on the boundary, and by linear superposition the net stresses and displacements will be obtained by suitably integrating the resulting expressions. In the contact of a rigid punch of any given shape with the half-space the problem is to find what pressure distribution acting within the actual contact area S will deform the plane such that its shape exactly matches the punch throughout S. This matching condition, it turns out, is sufficient to determine uniquely the bounding curve C of S as well as the pressure distribution within it; hence, the stress and strain may be found for any point in the half-space. In the absence of friction, the shear stress at the surface is everywhere zero.

To simplify the problem for illustrative purposes, we consider matching only the normal displacement component w, assuming that frictionless slip accommodates the radial movement u within the contact region required by the solution. The problem of matching radial displacements has been considered by Goodman (ref. 3). In the contact plane $z = 0$, equation (2c) becomes

$$\delta w = \frac{1}{\pi E'}\frac{p\,\delta S}{r}$$

(3)

by replacing F with $p\,\delta S$ and introducing the plane strain modulus $E' = E/(1-\nu^2)$. The net displacement at any point M in the contact plane can be found most easily by setting up the local polar coordinates (r, ϕ) shown in figure 2, since in this system $\delta S/r = \delta\phi\,\delta r$ is independent of the coordinates. Hence, we have

$$w_M = \frac{1}{\pi E'}\iint\limits_S p(r,\phi)\,dr\,d\phi$$

(4)

In the neighborhood of the contact, occurring at an extremum of the punch with respect to the contact plane, the shape may be written by suitably orienting axes in the general principal axis form
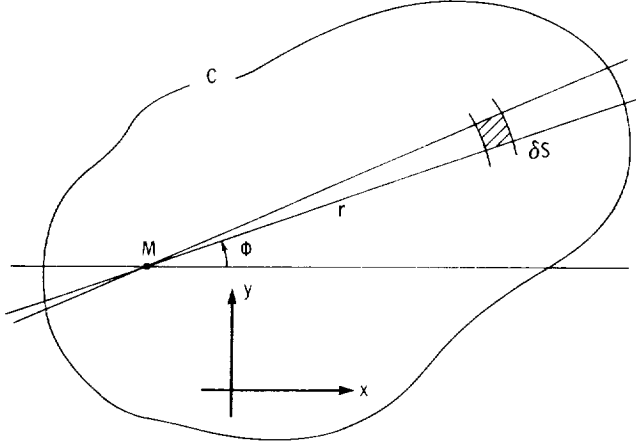
$$z_p = d - \frac{x^2}{2R_x} - \frac{y^2}{2R_y}$$

(5)

3

Figure 2.—Local polar coordinates in contact region of loaded elastic half-space showing contact bounding curve C.

where R_x and R_y are the two principal radii of curvature of the punch at the extremum and d is the penetration depth of this tip, lying on the z-axis. Later we will further assume $R_y > R_x$ so that the elliptical cross section has its major axis in the y-direction.

The projection of C on the contact plane is now assumed to be elliptical (C in general will not be a plane curve) with semiaxes (a,b) along (x,y) while the pressure distribution is semiellipsoidal:

$$p(x,y) = p_0 \left(1 - \frac{x^2}{a^2} - \frac{y^2}{b^2} \right)^{1/2} \tag{6}$$

Integrating p within C yields the total load F:

$$F = \frac{2}{3} p_0 \pi ab \tag{7}$$

so that the average pressure $F/\pi ab$ is just two-thirds of its central maximum value p_0. The consistent determination of (a,b) in terms of (R_x, R_y) constitutes a complete solution of this problem, since the stress tensor is then known in terms of various integrals within C. The solution also yields the penetration depth d which in the three-dimensional problem may be physically visualized as the depth of the tip of the indenter relative to the undeformed boundary of the half-space at large distances.

If M in equation (4) is the point (x,y),

$$w_M(x,y) = \frac{p_0}{\pi E'} \int\!\!\int_S \left[1 - \left(\frac{x + r\cos\phi}{a} \right)^2 - \left(\frac{y + r\sin\phi}{b} \right)^2 \right]^{1/2} dr\, d\phi \tag{8}$$

and the matching condition is simply

$$w_M(x,y) = z_p(x,y) \tag{9}$$

Performing the r integration first, the integrand may be cast in the standard form $[\alpha - 2\beta r - \gamma r^2]^{1/2}$ to yield

$$\frac{\beta + \gamma r}{2\gamma} [\alpha - 2\beta r - \gamma r^2]^{1/2} + \frac{\alpha\gamma + \beta^2}{2\gamma^{3/2}} \arcsin \frac{\beta + \gamma r}{(\alpha\gamma + \beta^2)^{1/2}}$$

The ϕ dependence of the coefficients (α,β,γ) is such that incrementing ϕ by π leaves α and γ invariant but changes the sign of β. Thus, at the lower limit $r = 0$, the coefficient ensures that the subsequent ϕ integration of both terms in the interval 0 to 2π will yield zero. At the upper limit of r, where the bracket vanishes, the arc sin gives $\pi/2$ and we are left with

$$w_M(x,y) = \frac{p_0}{4E'} \int_0^{2\pi} \frac{\alpha\gamma + \beta^2}{\gamma^{3/2}} d\phi \tag{10}$$

Examining next the (x,y) dependence of this remaining ϕ integrand, we find a term independent of (x,y) and terms quadratic in x and y, all of which are invariant when adding $\pi/2$ to ϕ. A fourth term, bilinear in x and y, changes sign. Taking advantage of this property and substituting for α and β give the result

$$w_M(x,y) = \frac{p_0}{E'} \int_0^{\pi/2} \left(\frac{1}{\gamma^{1/2}} - \frac{x^2}{a^2 b^2} \frac{\sin^2\phi}{\gamma^{3/2}} \right. \\ \left. - \frac{y^2}{a^2 b^2} \frac{\cos^2\phi}{\gamma^{3/2}} \right) d\phi \tag{11}$$

where $\gamma = (\cos^2\phi)/a^2 + (\sin^2\phi)/b^2$. This has precisely the functional form required by the matching condition (eq. (9)). Thus, the choices for C and $p(x,y)$ in equation (6) are self-consistent, and it at once becomes possible to determine the axes of the contact ellipse in terms of the principal radii of the indenter. To obtain these in standard form, we first introduce two notations:

$$\kappa \equiv b/a \tag{12}$$

$$\Delta \equiv \left[1 - \left(1 - \frac{1}{\kappa^2} \right) \sin^2\phi \right]^{1/2} = \frac{b}{\kappa} \gamma^{1/2} \tag{13}$$

It is always possible to satisfy $\kappa \geq 1$ by appropriately naming the (x,y) axes relative to the principal directions of the punch.

Comparing the terms in equations (5) and (11) shows the following relationships must hold:

4

|

$$\frac{1}{2R_x} = \frac{p_0}{E'} \frac{1}{\kappa b} \int_0^{\pi/2} \frac{\sin^2 \phi}{\Delta^3} d\phi = \frac{p_0}{E'} \frac{\kappa}{b} \int_0^{\pi/2} \frac{\cos^2 \phi}{\Delta} d\phi \quad (14)$$

$$\frac{1}{2R_y} = \frac{p_0}{E'} \frac{1}{\kappa b} \int_0^{\pi/2} \frac{\cos^2 \phi}{\Delta^3} d\phi = \frac{p_0}{E'} \frac{1}{\kappa b} \int_0^{\pi/2} \frac{\sin^2 \phi}{\Delta} d\phi \quad (15)$$

where the second form has been obtained by simple partial integration to yield the standard complete elliptic integrals B and D, as displayed in appendix A. The argument $(1 - \kappa^{-2})^{1/2}$ of these functions is just the eccentricity ϵ of the contact ellipse. Correspondingly, an expression for the penetration depth d is found from the term independent of (x,y) in equation (11):

$$d = \frac{p_0}{E'} \frac{b}{\kappa} \int_0^{\pi/2} \frac{1}{\Delta} d\phi \quad (16)$$

In this form d is clearly proportional to the elliptic integral $K(\epsilon)$.

To complete the solution it is necessary to determine the eccentricity ϵ, or equivalently κ, from the known principal curvatures of the indenter. In terms of the ratio $\alpha = R_y/R_x$, equations (14) and (15) may at once be solved for κ to give

$$\kappa = \left(\alpha \frac{D}{B} \right)^{1/2} \quad (17)$$

Substituting for the elliptic integrals B and D in favor of K and $\mathcal{E}_x$ gives

$$\kappa = \left[(\alpha + 1) \frac{K}{\mathcal{E}} - \alpha \right]^{1/2} \quad (18)$$

Alternative forms of equations (17) and (18) often appear in which the dimensionless ratio α is replaced by Γ defined as the ratio of the difference to the sum of the principal curvatures. Thus, if $R^{-1} \equiv R_x^{-1} + R_y^{-1}$ is the sum of the curvatures, then $\Gamma \equiv (R_x^{-1} - R_y^{-1})R$ and the equations for κ become, respectively,

$$\kappa = \left(\frac{1 + \Gamma}{1 - \Gamma} \frac{D}{B} \right)^{1/2} \quad (19)$$

and

$$\kappa = \left[\frac{2K - (1 + \Gamma)\mathcal{E}}{(1 - \Gamma)\mathcal{E}} \right]^{1/2} \quad (20)$$

From equation (5), a condition for the contact boundary C to be a plane curve is that the radius ratio α should be equal to the square of the axial ratio κ^2. Equation (17) however shows this can hold only if $B = D$, which occurs when $\epsilon = 0$, the special case of circular contact. In general C is not plane.

When the punch has penetrated to depth d beneath the surface $z = 0$, its elliptic cross section in this plane has semiaxes (a_0, b_0) given according to equation (5) by

$$\frac{a_0^2}{2R_x} = \frac{b_0^2}{2R_y} = d \quad (21)$$

From equations (14) to (16) the semiaxes of C satisfy the relation

$$\frac{1}{2R_x} a + \frac{1}{2R_y} \frac{b^2}{a} = d \frac{1}{a} \quad (22)$$

which in combination with equation (21) leads to the interesting and perhaps unanticipated result

$$\frac{a^2}{a_0^2} + \frac{b^2}{b_0^2} = 1 \quad (23)$$

This simple expression is useful in avoiding the pitfall of setting $(a,b) = (a_0, b_0)$. In the $y = 0$ plane, this distinction between a and a_0 is shown graphically in figure 3.

Adding equations (14) and (15) and substituting the total load F from equation (7) yield an explicit expression for the semimajor axis of C:
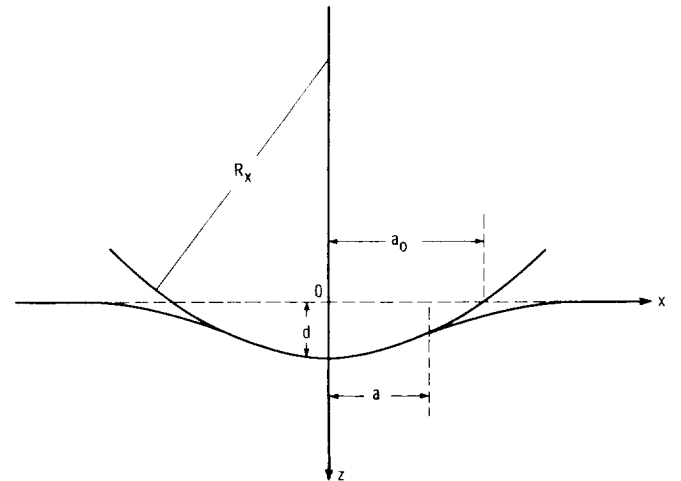

Figure 3.—In $y = 0$ plane, ellipsoidal punch appears approximately circular with radius R_x. Its intercept at $x = a_0$ with initial contact plane $z = 0$ is compared with contact semiaxis a.

5

$$b = \left[\frac{3F\kappa^2 R}{\pi E'}(B + D/\kappa^2)\right]^{1/3} = \left(\frac{3F\kappa^2 R\mathcal{E}}{\pi E'}\right)^{1/3} \qquad (24)$$

The semiminor axis $a = b/\kappa$ then becomes

$$a = \left(\frac{3FR\mathcal{E}}{\pi\kappa E'}\right)^{1/3} \qquad (25)$$

while the penetration depth d is given by

$$d = \frac{K}{2\mathcal{E}R}\left(\frac{3FR\mathcal{E}}{\pi\kappa E'}\right)^{2/3} = \frac{K}{2\mathcal{E}R}a^2 \qquad (26)$$

Since κ and R are fixed by the geometry of the rigid indenter, independent of load, it follows from equations (24) to (26) that the linear dimensions of the contact ellipse grow as the one-third power of the load, while the penetration depth accordingly increases as the two-thirds power.

For given α, equation (17) or its equivalents (eqs. (18) to (20)) are transcendental equations for κ which may readily be solved, for example, by iteration. When α is only slightly greater than unity, ϵ is small and the expansions of the elliptic integrals given in appendix A may be used to obtain a closed solution. If this is written in the form

$$\kappa = \alpha^n \qquad (27)$$

and only the first two terms in the expansions are used, the exponent n is easily found to be 2/3. Comparing equation (27) with direct numerical evaluation of κ shows this approximation to be surprisingly accurate, with, for example, an error of only 3 percent for α as large as 10. For such a radius ratio, $\epsilon = 0.97$ so that the accuracy of equation (27) clearly far exceeds that of the approximations used for the elliptic integrals.

In a more exhaustive investigation of the $\kappa(\alpha)$ relationship, Hamrock and Brewe (ref. 4) used linear regression to fit equation (27) over the larger range $1 \le \alpha \le 100$. They find the least squares value of n to be $2/\pi$, only some 5 percent smaller than the limiting value, which yields a maximum error in κ of less than 4 percent for their larger range.

For the special case of a spherical punch of radius R_0, the preceding general analysis is more complicated than necessary. The final result, however, is derived readily from the general case by setting $R = R_0/2$ and $\Gamma = 0$. Equation (17) then gives $\kappa = 1$ since when argument $(1 - \kappa^{-2})^{1/2} = 0$ integrals B and D both have the value $\pi/4$

and K and $\mathcal{E}$ both equal $\pi/2$. The radius of the circular contact (eq. (24) or (25)) and the penetration depth (eq. (26)) become

$$a = \left(\frac{3FR_0}{4E'}\right)^{1/3} \qquad (28)$$

and

$$d = 2\frac{1}{2R_0}\left(\frac{3FR_0}{4E'}\right)^{2/3} = 2\frac{a^2}{2R_0} \qquad (29)$$

These results are the more familiar Hertz expressions, written to show that the plane edge of the circular contact occurs at a depth of exactly $d/2$. The actual contact area at this level is consequently just half the cross section area of the punch at the level of initial contact, $z = 0$, which also follows directly from equation (23).

Equations (24) to (26) together with equation (17) furnish a complete and rigorous solution of the contact problem for a rigid indenter of arbitrary shape on an elastic half-space. Substituting the contact pressure (eq. (6)) into equations (1) and (2) and integrating over the contact region give the stress tensor and corresponding elastic displacements at the general internal field point, including the plane of initial contact itself. Such calculations were first carried out for circular contact by Huber (ref. 5) in 1904. The general elliptic contact was not analyzed until 1917 by Belajef (ref. 6), almost four decades after Hertz' solution for the surface stresses. Somewhat later, Thomas and Hoersch (ref. 7) obtained the stress components on the axis of symmetry as a function of the eccentricity of the contact ellipse ϵ. Such calculations allow the principal and octahedral shear stresses to be found; the absolute maxima of these stresses determine the initial yield point of the half-space according, respectively, to the criteria of Tresca or von Mises. The position of the maximum principal shear stress, for example, rises from a depth of $0.78a$ beneath the surface when $\epsilon = 1$ (line contact) to $0.57a$ when $\epsilon = 0$ (circular contact), taking ν to be 0.3. The magnitude of this stress is, however, insensitive to ϵ, varying only from $0.30p_0$ in line contact to $0.31p_0$ in circular contact.

Another feature of interest appears in the radial stress component σ_ρ which at the surface changes sign from compressive at contact center to tensile just inside the contact edge. In circular contact this component ranges from $-0.8p_0$ at the center to $0.133p_0$ at the edge itself. For brittle materials, failure is initiated at such points of maximum tensile stress. Furthermore, since the circumferential stress σ_θ remains compressive, equal but opposite to σ_ρ outside the contact circle, the maximum shear stress in the surface is quite appreciable. These

stresses fall monotonically to zero as the inverse square of the distance.

Extensions of Point Contact

In most practical applications of this mechanical analysis, the axes of the contact ellipse are several orders of magnitude smaller than the radii of curvature of the indenter; therefore, the solution may be extended to cover a wider class of contact problems. Since elastic displacements decrease as $1/r$ (see eq. (2)), both bodies are then sufficiently flat within the region where displacements are significant so that it is immaterial whether one or both of the bodies have curvature and whether one or both are deformable. The gap between the bodies (given by eq. (5)) becomes the sum of the two separate deviations from the $z=0$ plane, and it is thus necessary only to express the gap in principal axis form. If the principal axes of the two bodies are aligned, a common situation, then, with a suitable convention for the signs of radii, this is achieved by writing $1/R_x = (1/R_x)_1 + (1/R_x)_2$ and likewise for the y-curvatures. Similarly, the elastic displacements of the bodies (given by eq. (8)) are summed and $1/E'$ may simply be replaced by $1/E_1' + 1/E_2'$. **Caution:** A convention is sometimes used whereby $1/E'$ is defined as $(1/E_1' + 1/E_2')/2$, which has certain appeal when both bodies are of the same material; however, if this convention is adopted, then in the preceding work, E' must be replaced by $E'/2$. Some of the most useful results derived in this section for three-dimensional contact are displayed in tables I(a) and (b) at the back of the report (pp. 21 and 22).

Reduction of the Fundamental Solution

In the previous section the solution for a point force F was developed to handle distributed pressure problems by replacing F with $p\,\delta S$. A corresponding replacement of F by $q\,\delta l$ allows a treatment of a concentrated line force of magnitude q per unit length acting normal to the half-space along line element δl. If q is constant and the entire y-axis acts as the line, an integration of equation (1) yields a stress tensor independent of the y-coordinate. Because the ρ- and θ-directions used in equation (1) are referenced to each source element, it is convenient to transform the tensor to Cartesian form before carrying out the integration. Then, the ρ- and θ-coordinates of the field point M taken in the $y=0$ plane with respect to source F on the y-axis are as shown in figure 4. The required tensor transformation, taking account of the zero components in the original cylindrical system, becomes
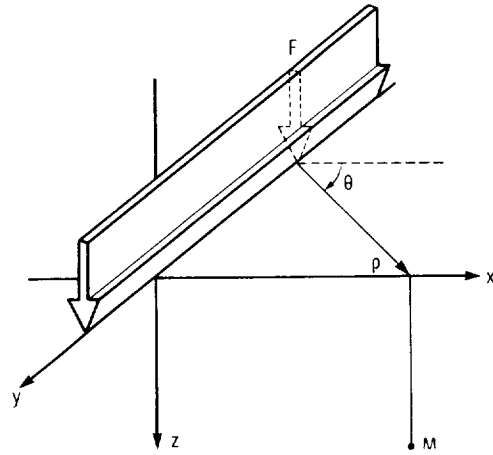

Figure 4.—Coordinates of field point M with respect to point force F acting on y-axis.

$$\sigma_x = \sigma_\rho \cos^2 \theta + \sigma_\theta \sin^2 \theta$$

$$\sigma_y = \sigma_\rho \sin^2 \theta + \sigma_\theta \cos^2 \theta$$

$$\tau_{xy} = \frac{1}{2}(\sigma_\rho - \sigma_\theta) \sin 2\theta$$

$$\tau_{xz} = \tau_{\rho z} \cos \theta$$

$$\tau_{yz} = \tau_{\rho z} \sin \theta$$

$$\sigma_z = \sigma_z$$

$$(30)$$

From symmetry it is clear that τ_{xy} and τ_{yz} vanish upon integration, but for the remaining components no way has been found to avoid actually carrying out the rather lengthy integrations. The results depending only on (x,z) may be more clearly expressed in terms of the (R,ψ) coordinates of figure 1:

$$\sigma_x = -\frac{2q}{\pi R} \sin^2 \psi \cos \psi$$

$$\sigma_y = -\frac{2\nu q}{\pi R} \cos \psi$$

$$\tau_{xy} = 0$$

$$\tau_{xz} = -\frac{2q}{\pi R} \sin \psi \cos^2 \psi$$

$$\tau_{yz} = 0$$

$$\sigma_z = -\frac{2q}{\pi R} \cos^3 \psi$$

$$(31)$$

7

It follows that these equations describe a state of plane strain since $\sigma_y = \nu(\sigma_x + \sigma_z)$ and $\tau_{xy} = \tau_{yz} = 0$. Note also that the only role of the Poisson ratio in this quasi-two-dimensional solution is to generate a normal stress in the excluded y-dimension just sufficient to maintain zero y strain. The more important involvement of ν in the original three-dimensional solution of equation (1) is required by the compatibility relations.

Having expressed the Cartesian stress components in polar coordinates, it is clear what their cylindrical polar counterparts are. By inspection, all components in this representation are zero except for σ_R and σ_y:

$$\left.\begin{array}{l} \sigma_R = -\dfrac{2q}{\pi R} \cos \psi \\[4mm] \sigma_y = -\dfrac{2\nu q}{\pi R} \cos \psi = \nu \sigma_R \end{array}\right\} \qquad (32)$$

Thus, in the y-plane, this somewhat lengthy analysis has reduced the stress system to a single radial compressive stress (with no shear). This system is so simple that it is often used as the starting point in elementary treatments. The displacements produced by this stress system may be found, like the stresses, by integrating the three-dimensional result, but it is actually easier to derive them directly from the stresses of equation (32). Neither approach avoids the problem of the logarithmic divergences of the displacements at $R \to 0$ and $R \to \infty$. The former coincides with the singularity in the stress so that it makes physical sense to excise a small region around the origin in the same manner as for the three-dimensional solution. The divergence at large distances in regions which are stress-free is somewhat more troublesome, since it deprives the solution of an undisplaced region of the contact plane to serve as the natural reference level for displacements. Instead, a finite datum point is forced on the solution and its choice affects the form, if not the content, of subsequent expressions for various displacements of interest.

In the cylindrical system of equation (32) one useful form of the displacement components (u,v,w) in the (R,y,ψ) directions may be written

$$\left.\begin{array}{l} u = -\dfrac{q}{\pi E'} \left(2 \cos \psi \ln \dfrac{R}{d_0} + \dfrac{1-2\nu}{1-\nu} \psi \sin \psi \right) \\[4mm] v = 0 \\[4mm] w = \dfrac{q}{\pi E'} \left(2 \sin \psi \ln \dfrac{R}{d_0} - \dfrac{1-2\nu}{1-\nu} \psi \cos \psi + \dfrac{\sin \psi}{1-\nu} \right) \end{array}\right\} \qquad (33)$$

again showing that this is plane strain. The parameter d_0 is chosen as the reference depth beneath the surface $z = 0$ at which the displacement in the symmetry plane $x = 0$ vanishes. The azimuthal component w has been made antisymmetric about this plane.

Contact In Two Dimensions

Rigid Cylinder and Elastic Half-Space

For contact problems the important part of the solution is again the normal (downward) displacement of the original bounding surface $z = 0$, given in this case by

$$w(R, -\pi/2) = -w(R, \pi/2) =$$

$$-\dfrac{2q}{\pi E'} \left[\ln \dfrac{R}{d_0} + \dfrac{1}{2(1-\nu)} \right] \qquad (34)$$

This is applied first to the contact of a rigid cylindrical punch with an elastic half-space, where initial contact is along a generator touching the y-axis. If only normal displacements are matched, the technique follows exactly that for frictionless point contact. An x-dependent pressure distribution $p(x)\,dx$ replaces the line force q and the integral of equation (34) is matched to the azimuthal cross section of the indenter. Shear stresses in the initial contact plane are again zero. The choice for $p(x)$, guided by equation (6), is taken to be the semielliptical distribution

$$p(x) = p_0 \left(1 - \dfrac{x^2}{a^2} \right)^{1/2} \qquad (35)$$

so that the total load per unit length is just

$$q = \dfrac{\pi}{2} p_0 a \qquad (36)$$

The resultant z-component of the displacement in the $z = 0$ plane then becomes

$$-w(x) = \dfrac{2q}{\pi E'} \left[\ln d_0 - \dfrac{1}{2(1-\nu)} \right]$$

$$-\dfrac{2p_0}{\pi E'} \int_{-a}^{a} \left(1 - \dfrac{x'^2}{a^2} \right)^{1/2} \ln |x - x'| \, dx'$$

or, expressing the integral in standard form,

$$-w(x) = \frac{2q}{\pi E'} \left[\ln \frac{d_0}{a} - \frac{1}{2(1-\nu)} \right]$$

$$- \frac{2p_0 a}{\pi E'} \int_{-1}^{1} (1 - x'^2)^{1/2} \ln \left| \frac{x}{a} - x' \right| dx' \qquad (37)$$

When combining equation (34) with the pressure distribution of equation (35), r becomes the distance between the pressure element and the field point, which accounts for the appearance of the modulus of the relative coordinate in the integral. Similarly, d is the distance between the pressure element and the datum point so that equation (34) requires generalization to accommodate an arbitrary datum before incorporation with the distributed pressure. On the assumption, however, that the datum is chosen at a distance large compared to the extent of the contact pressure, the variation of this distance has been neglected in arriving at equation (37). In the three-dimensional case, the reference point is taken at infinity and this consideration never explicitly arises.

The remaining integrand in equation (37) is singular for points within the contact strip flanking the y-axis out to distance a on either side. Taking the Cauchy principal value for the integral as indicated by the modulus sign leads to the following closed forms:

$$\int_{-1}^{1} \left(1 - x'^2\right)^{1/2} \ln \left| \frac{x}{a} - x' \right| dx'$$

$$= \frac{\pi}{2} \left(-\ln 2 - \frac{1}{2} + \frac{x^2}{a^2} \right) \qquad |x| \le a \qquad (38a)$$

$$\int_{-1}^{1} \left(1 - x'^2\right)^{1/2} \ln \left| \frac{x}{a} - x' \right| dx' = \frac{\pi}{2} \left\{ -\ln 2 - \frac{1}{2} + \frac{x^2}{a^2} \right.$$

$$+ \ln \left[\frac{|x|}{a} + \left(\frac{x^2}{a^2} - 1 \right)^{1/2} \right]$$

$$\left. - \frac{|x|}{a} \left(\frac{x^2}{a^2} - 1 \right)^{1/2} \right\} \qquad |x| > a \qquad (38b)$$

As before, the contact dimension must be determined by matching the displaced surface to the indenter shape within the contact region. Corresponding to equation (5), if R_x is the radius of curvature of the indenter at the point of initial contact, then the local shape in general is given by

$$z_p = d - \frac{x^2}{2R_x} \qquad (39)$$

For two-dimensional contact, radius R_x becomes identical with radius R, defined previously as the reciprocal of the sum of the x- and y-curvatures. We shall therefore suppress the x subscript in subsequent expressions referring to two-dimensional cases. The displaced surface according to equations (36) to (38) may now be written

$$-w(x) = \frac{2q}{\pi E'} \left(\ln \frac{2d_0}{a} - \frac{\nu}{2(1-\nu)} - \frac{x^2}{a^2} \right) \quad |x| \le a \qquad (40)$$

which matches equation (39) in form. The assumed pressure distribution is thus consistent and may be made to fit the physical conditions of this problem by choosing the contact semiwidth a and penetration depth d to be

$$a = 2 \left(\frac{Rq}{\pi E'} \right)^{1/2} \qquad (41)$$

$$d = \frac{2q}{\pi E'} \left[\ln \frac{2d_0}{a} - \frac{\nu}{2(1-\nu)} \right] \qquad (42)$$

These results correspond to the three-dimensional expressions given in equations (24) to (26) and show that the linear size of the contact zone increases here as the $1/2$ power of the load per unit length. The penetration depth increases essentially linearly with load except, as equation (42) shows, there is also a weak logarithmic dependence from the appearance of a in the bracket. Because of the freedom of choice for the reference depth d_0, no particular relationship exists between a and d which would correspond to equations (26) or (29) for point contact.

Characteristically, d_0 might be assigned a value comparable to R. A typical example of the effect of choosing different reference positions may be given by shifting the datum from $(x,z) = (0,d_0)$, a depth d_0 beneath the indenter, to $(d_0,0)$, a distance d_0 to the side in the original undisplaced surface. Reexpressing the displacements of equation (33) in accordance with this new choice leads to $+1/2$ in place of the term $-\nu/2(1-\nu)$ within the bracket of equation (42) for d.

As the distance $|x|$ from the contact zone increases, equations (37) and (38) show that the normal surface displacement increases without limit as $\ln (|x|/d_0)$ in the direction opposite to that of the applied force. Such behavior is of course expected from the discussion of the fundamental displacements given in connection with equation (33).

With the contact width known as a function of load, the rigid punch problem can now be solved completely for stress and strain tensors by appropriate combination

of the pressure distribution of equation (35) with the basic line force solution (eqs. (31) and (33)). The first to perform such calculations were Huber and Fuchs (ref. 8), while more recently, elegant solutions have been provided by Poritsky (ref. 9) and Smith and Liu (ref. 10). In appendix B, the straightforward integration of equation (31) leads directly to the stress tensor given by equation (B15). Plots of these stress intensities are presented in figures (6) to (8) while some special cases of interest are discussed here in more detail.

Consider first the surface of the half-space $\zeta = 0$. From equation (B12) it follows that $\alpha^2 = \pm(\xi^2 - 1)$ where the choice of sign must be determined by the requirement that β be real in equation (B11). This leads to $\alpha^2 = 1 - \xi^2$ when $\xi^2 < 1$ (inside the contact zone) and $\alpha^2 = \xi^2 - 1$ when $\xi^2 > 1$ (outside the contact zone), so that the actual value of α^2 is never negative. Correspondingly, $\beta = (1 - \xi^2)^{1/2}$ inside and zero outside. When the surface is approached by taking $\lim \zeta \to 0$, the stress components are all found to vanish for points external to the contact region. Internal to the contact region, only the shear stress τ_{xz} is zero, while the normal stresses σ_x and σ_z are equal to each other and given by

$$\sigma_x = \sigma_z = -p_0\left(1 - \xi^2\right)^{1/2} \tag{43}$$

The z-component, of course, is just the contact pressure (eq. (35)), which is one of the boundary conditions of the model, but the x-component is perhaps unexpected. It produces a state of two-dimensional uniform (hydrostatic) compression in the surface layer, as a comparison of figures 6 and 8 also reveals. While the vanishing of σ_z and τ_{xz} on the surface outside the contact zone are also boundary conditions of the model, the vanishing of σ_x is not a requirement and again contributes some new information to the contact problem. In fact, this behavior of σ_x in two dimensions contrasts strongly with the behavior of the three-dimensional contact discussed earlier, where the corresponding normal component of stress in the radial direction actually reversed sign and became tensile just inside the contact boundary.

Another special case of interest is found by setting $\xi = 0$ to obtain the internal stress components on the symmetry axis of the indenter. In this case, $\alpha = \beta = (1 + \zeta^2)^{1/2}$. Again the shear stress τ_{xz} vanishes, as we expect by symmetry. The nonzero normal components are given by

$$\left.\begin{aligned} \sigma_x &= -\frac{p_0}{(1 + \zeta^2)^{1/2}}\left[2\zeta^2 + 1 - 2\zeta(1 + \zeta^2)^{1/2}\right] \\[2mm] \sigma_z &= -\frac{p_0}{(1 + \zeta^2)^{1/2}} \end{aligned}\right\} \tag{44}$$

which are plotted in figure 5. The normal stress σ_y, equal to ν times the sum of σ_x and σ_z, is also shown, again for the value of $\nu = 0.3$. At large depths these components display explicitly the $1/\zeta$ distance dependence characteristic of the plane strain condition.

Now that the normal stresses are no longer equal, the maximum shear stress τ_m lies in planes bisecting the x-and z-directions with a magnitude of $|\sigma_z - \sigma_x|/2$. This component is displayed in figure 5, which shows the previously noted maximum value of $0.3p_0$ at a depth approximately three-fourths of the Hertz semiwidth a, the initial yield point. By contrast, since τ_m vanishes everywhere at the boundary, the material immediately adjacent to the indenter is dead and not expected to flow.

Extensions of Line Contact

Extension of the analysis to cases where both contacting members have curvature and elasticity is less trivial in two than in three dimensions, when it sufficed simply to introduce a composite curvature and elastic modulus for the pair. The validity of this simple adaptation rested directly on the effective vanishing of the displacement in regions where curvature produced significant departure of either undeformed body from the ideal plane assumed for the basic solution. In two dimensions no part of this surface remains undisplaced so that the procedure of transferring curvature from one side to the other, known as bending the gap, represents at best a crude approximation which might be expected to break down in some situations.

Consider first the contact of an elastic cylinder with a rigid plane, the inverse of the situation described by the fundamental solution. If E' and ν now refer to the cylinder, then equation (41) still gives a good approximation to the contact width provided as always this turns out to be small compared with R. In the
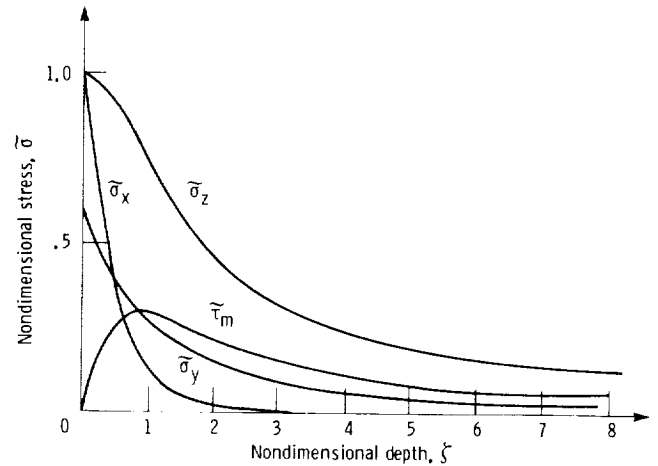

Figure 5.—Stress components for points along indenter axis internal to elastic half-space. Both distance and stress are given in nondimensional forms defined by equations (B1) and (B2).

expression for d (eq. (42)), however, the depth d_0 is now measured in the cylindrical body rather than in the half-space, and at distances $d_0 \sim R$ from the contact the shape of the cylinder may depart significantly from that of the half-space. Moreover, the parabolic form of equation (39) is often taken to approximate a circular roller, in which case the infinite half-space has been bent into a space finite in two dimensions. This emphasizes the nature of the approximations involved and the need to exercise judgment in selecting a datum. A natural choice in such cases is to fix the center of curvature by setting $d_0 = R$, whereupon the distance d of equation (42) becomes the shortening δR of the radius in the direction of the applied force q:

$$\delta R \approx \frac{2q}{\pi E'} \left[\ln \frac{2R}{a} - \frac{\nu}{2(1 - \nu)} \right] \tag{45}$$

The *approximately equals* sign in equation (45) is a reminder that this estimate of δR rests on the as yet untested bending hypothesis. A more accurate expression is presented in equation (47) based on an elastic solution for the line force acting on a circular cylindrical surface.

For parallel contact of two different cylinders, it follows from equations (39) and (40) that the contact semiwidth a may still be obtained from equation (41), as in three dimensions, by interpreting R^{-1} as $(R_1^{-1} + R_2^{-1})$ and E'^{-1} as $(E_1'^{-1} + E_2'^{-1})$. To find the approach of centers, however, these variables alone are insufficient because of the appearance of R and ν in equation (45) referring individually to each cylinder. The compliance is most clearly expressed just by adding the individual δR values in which, of course, a and q are common. Reduction to a single equivalent roller and flat is, in this respect, no longer particularly simple.

For the diametral reduction of a roller in compression between two parallel rigid flats, it is merely necessary to double the right side of equation (45). If the flats themselves are elastic, however, a little care is required first to substitute appropriate composite variables when finding a and second to appreciate that if the flats are of dissimilar materials, the two contact widths will not be equal. Thus, diametrically opposed radii are shortened by different amounts whose sum gives the net compliance.

As a final application, this analysis will be used to demonstrate its own limitations in treating the deformation of any body other than the half-space. Consider again the preceding example of the diametral compliance of a cylinder between rigid flats. If the gap bending hypothesis is correct, the analysis should yield a diametral compliance independent of the arbitrary reference point. Let this datum be chosen some distance $l < R$ from the midplane along the shortened diameter. Then, according to equation (42), the compliance δD

obtained by summing the decrements of the two segments will be

$$\delta D = 2 \frac{2q}{\pi E'} \left\{ \left[\ln \frac{2}{a} - \frac{\nu}{2(1 - \nu)} \right] + \frac{1}{2} \left[\ln (R + l) + \ln (R - l) \right] \right\}$$
$$= \frac{4q}{\pi E'} \left[\ln \frac{2R}{a} - \frac{\nu}{2(1 - \nu)} + \frac{1}{2} \ln \left(1 - \frac{l^2}{R^2} \right) \right] \tag{46}$$

This expression has explicit, though weak, dependence on the datum via l. Yet another result is obtained if $d_0 = 2R$ is inserted directly in equation (42). Use of the bending hypothesis for two-dimensional problems involving compliance is thus generally inaccurate or even inconsistent (ref. 11).

A resolution of this difficulty is to begin with a different basic elastic solution applying directly to curved bodies. One such solution, for a circular cylinder loaded by two equal and opposite line forces acting at the ends of a chord, has been given (ref. 12) and used in a contact analysis (ref. 13). This leads again to the pressure distribution of equation (35) in which the contact semiwidth a of equation (41) is, however, reduced slightly by the appearance of the factor $(1 + 2q/\pi E' R)$ in the denominator. From the discussion of equation (42) it might be expected that the effect of the exact solution on d would be seen chiefly in the second term in the bracket, already shown to be sensitive to choice of datum. Thus, in addition to requiring the new expression for a in the first term, the rigorous solution also replaces $-\nu/2(1 - \nu)$ by $(\ln 2 - 1/2)$:

$$\delta R = \frac{2q}{\pi E'} \left[\ln \frac{2R}{a} + \left(\ln 2 - \frac{1}{2} \right) \right] \tag{47}$$

Setting $a/R = 10^{-n}$, the fractional error in the earlier approximation for a amounts to $(10^{-n}/2)^2$ whereas for δR given in equation (45) it is far larger, roughly $-0.2/n$ for typical values of ν. In practical situations n could be as small as 2; thus, in the worst case, application of plane Hertz theory to a cylinder overestimates a by a negligible 0.0025 percent but underestimates δR by as much as 10 percent.

It may be seen then that the gap bending conjecture works well in determining contact widths but encounters difficulties in predicting compliances where the arbitrary datum is involved. From this it is perhaps not surprising that the contact semiwidth of equation (41) may be found as the appropriate limit of equation (25) for the semiminor axis in three-dimensional contact, whereas the

corresponding link between compliances in two- and three-dimensional situations does not exist. The connection between line and point contact loaded to the same maximum pressure p_0 may be established by eliminating p_0 between equations (7) and (36) to obtain

$$q = \frac{3}{2}\frac{F}{2b} \tag{48}$$

As R_y increases without limit, so $\Gamma \rightarrow 1$, $\kappa \rightarrow \infty$, $\mathcal{E} \rightarrow 1$, and $K \rightarrow \ln 4\kappa$. To maintain a finite load per unit length of the elongated contact ellipse, the total load F also diverges while satisfying equation (48). Substituting these limiting values in equation (25) yields the correct two-dimensional result for the contact semiwidth (eq. (41)). However, while the corresponding limit of equation (26) correctly predicts a logarithmic divergence in the two-dimensional compliance, it clearly cannot be used to introduce a datum level d_0. Tables II(a) and (b) exhibit graphically a number of the more important results of this section on two-dimensional contact problems (see pp. 23 and 24).

Line Contact of Real Surfaces

A further interesting development of two-dimensional contact analysis was carried out by McCallion and Truong (ref. 14) when they investigated the effect of surface roughness on the load-compliance relation for a rough cylinder between smooth flats. As a model of the pressure produced by the asperity layer they used the family of contact pressures given by

$$p = p_0 \left(1 - \frac{x^2}{a^2}\right)^\beta \qquad |x| < a \tag{49}$$

acting in opposition over a band at each end of a diameter of the circular cylinder. The contact analysis is based on the elastic solution for diametrically opposed line forces acting on a cylinder (see appendix C) so that it is limited to $a/R \ll 1$ from the outset. The standard integral corresponding to that of equation (38) now appears with the variable exponent β in place of $1/2$ but, again provided $a/R \ll 1$, the diametral compression can still be evaluated in closed form. The result equivalent to equation (45) is found to be

$$\delta R = \frac{2q}{\pi E'} \left\{ \ln \frac{2R}{a} + \ln 2 - \frac{\beta}{\beta + 1/2} \right.$$
$$\left. + \frac{1}{2}\left[\psi(\beta + 1/2) + \gamma\right] \right\} \tag{50}$$

As with the effect of transferring curvature from the rigid to the elastic contact member, the effect of changing the distribution of load within the narrow band of width $2a$ is confined to the second term of equation (42). For the special case $\beta = 1/2$ required by the matching condition in smooth contact, $\psi(1) = -\gamma$ and this second term reduces to $\ln 2 - 1/2$ in agreement with the result shown earlier (eq. (47)).

At this point a number of results for the compliance of a cylinder and flat configuration have been derived, such as those found in equations (42), (47), and (50). The important differences in these expressions are determined by which of the two contacting members possesses curvature or elasticity, by choice of the datum, or by distribution of contact pressure. Further modification may be produced by matching tangential displacements as part of the condition of contact. Continuing in this vein, a paper by Nikpur and Gohar (ref. 15) exhibits no fewer than nine different compliance formulae extracted from the literature for comparison with a tenth expression based on their own experimental data. Beyond a number of purely numerical errors, probably arising from notational difficulties, most of the apparent conflicts between theories clearly arise from genuine differences in the mathematical models. These are precisely the type under consideration herein, concerned with whether to include compliance of the platens, where to fix the datum if this is included, what contact pressure to use, and so forth.

Although all ten expressions predict a compliance increasing with applied load, as required for mechanical stability, there is no such agreement for the dependence on cylinder radius which ranges from monotonic increasing to constant and even to decreasing. Despite this, the work of reference 14 does illustrate a further important point beyond simply the need to recognize what assumptions are built into a given model. This sometimes overlooked point concerns the physical validity of the assumptions themselves under the actual conditions of measurement. The behavior of a real surface often turns out to be rather different from that of its ideal, smooth, isotropic counterpart (ref. 16), demanding considerable skill and ingenuity in the construction of faithful rather than merely solvable mathematical models. It is this fact which continues, some 100 years after the Hertz analysis, to justify both theoretical and experimental studies of such an apparently straightforward mechanical system.

Conclusions

One objective of this review has been to examine some of the assumptions entering into the analysis of

mechanical contact between elastic bodies. Particular emphasis has been placed on reducing three-dimensional solutions to quasi-two-dimensional situations where elementary metric properties of space introduce difficulties by virtue of the logarithmic divergence of elastic displacements with distance from the contact. The variety of forms this permits for the compliance of contacting bodies in two dimensions underlines the need to exhibit unambiguously the assumptions on which each rests.

The application of plane Hertz theory to the displacement of cylindrical surfaces is based on the gap bending hypothesis which asserts that the effect of geometry on mechanical conditions in the contact region is determined entirely by the algebraic sum of the curvatures of the two contacting bodies. Stated another way, contact between two curved surfaces can always be reduced to contact between a plane and an equivalent curved surface, whose curvature is the sum of the two original curvatures. Predictions of plane Hertz theory applied to cylinders have been compared to those of an analysis based on exact solutions for the displacement of cylindrical surfaces by a line force. As with its optical counterpart in lens theory, the bending conjecture produces results of mixed quality. Thus, in two dimensions, the contact width is predicted with high accuracy but the hypothesis breaks down for the compliance, resulting in errors in practical cases as large as 10 percent. If for a particular application only the contact width and the semielliptical pressure distribution are required, then, as argued by Johnson, the errors introduced by the plane Hertz approximation are of comparable magnitude with errors incurred by using linearized elasticity theory, and the extra effort required by the refined solution is hardly justified. In matters involving compliance, however, the argument is invalid and it becomes important to improve on the plane elastic solution, if for no other reason than to provide at least some error estimate of the initial approximation.

While the elastic analysis presented herein should be sufficiently general to allow modification appropriate to any configuration, it nevertheless seems worthwhile to collect some of the more common results together for easy reference. Accordingly, tables are included as a useful and illustrative summary of the principal results of this review.

Appendix A
Complete Elliptic Integrals

General Definitions

A general complete elliptic integral is defined by the expression

$$J(k) \equiv \int_0^{\pi/2} \frac{\Phi}{\Delta} d\phi$$

where $\Delta = (1 - k^2 \sin^2 \phi)^{1/2}$. For particular forms of Φ, the conventional notation is as follows:

Φ	Notation
$\cos^2 \phi$	B
$\sin^2 \phi$	D
Δ^2	$\mathcal{E}$ (second kind)
1	K (first kind)

Only two of these elliptic integrals are independent since it is clear that $B + D = K$ and $B + (1 - k^2)D = \mathcal{E}$. The argument of the elliptic integrals appearing in equations (17) to (20) and (24) to (26) is given by $k = \epsilon$ where $\epsilon = (1 - \kappa^{-2})^{1/2}$ is the eccentricity of the contact ellipse.

Series Expansions

For ϵ very small (nearly circular contact):

$$\frac{4}{\pi} B = 1 + \frac{1}{8} \epsilon^2 + \frac{3}{64} \epsilon^4 + \dots$$

$$\frac{4}{\pi} D = 1 + \frac{3}{8} \epsilon^2 + \frac{15}{64} \epsilon^4 + \dots$$

$$\frac{2}{\pi} \mathcal{E} = 1 - \frac{1}{4} \epsilon^2 - \frac{3}{64} \epsilon^4 - \dots$$

$$\frac{2}{\pi} K = 1 + \frac{1}{4} \epsilon^2 + \frac{9}{64} \epsilon^4 + \dots$$

For κ very large (long, narrow elliptical contact):

$$B = 1 - \frac{1}{2} \left(\Lambda - \frac{3}{2} \right) \kappa^{-2} - \dots$$

$$D = (\Lambda - 1) + \frac{3}{4} \left(\Lambda - \frac{4}{3} \right) \kappa^{-2} + \dots$$

$$\mathcal{E} = 1 + \frac{1}{2} \left(\Lambda - \frac{1}{2} \right) \kappa^{-2} + \dots$$

$$K = \Lambda + \frac{1}{4} (\Lambda - 1) \kappa^{-2} + \dots$$

where $\Lambda = \ln 4\kappa$.

Appendix B
Stress Tensor for Indentation of Elastic Half-Space by Rigid Cylindrical Punch

Equation (31) represents the stress tensor for a concentrated normal line load q on the surface of an elastic half-space, using the coordinates of figure 1(b). In plane strain, two of the shear components vanish while the normal stress in the suppressed direction is just ν times the sum of the other two normal stresses, leaving only three components to solve for. Under contact conditions, the line force q is replaced by the pressure $p(x)$ given by equation (35) acting over the infinitesimal width dx, the net result being expressed as the integral over the whole contact region where $p(x)$ is nonzero.

Coordinates (R,ψ) are relative to the position of the element dx so that the natural system to use is the Cartesian system of figure 1(b). Introducing the nondimensional coordinates

$$\left. \begin{aligned} \xi &= \frac{x}{a} \\[2mm] \zeta &= \frac{z}{a} \end{aligned} \right\} \tag{B1}$$

and the nondimensional stress tensor

$$\tilde{\sigma} = \frac{\sigma}{p_0} \tag{B2}$$

the integrals for the three components of interest become

$$\begin{pmatrix} \tilde{\sigma}_x(\xi,\zeta) \\[3mm] \tilde{\tau}_{xz}(\xi,\zeta) \\[3mm] \tilde{\sigma}_z(\xi,\zeta) \end{pmatrix} = -\frac{2}{\pi} \int_{-1}^{1} \frac{(1-\xi'^2)^{1/2}}{R^4} \begin{pmatrix} (\xi-\xi')^2\zeta \\[3mm] (\xi-\xi')\zeta^2 \\[3mm] \zeta^3 \end{pmatrix} d\xi' \tag{B3}$$

where now $R^2 = (\xi - \xi')^2 + \zeta^2$.

The integrals involved here may all be evaluated from the single integral

$$I_1(\xi,\zeta) = \int_{-1}^{1} \frac{(1-\xi'^2)^{1/2}}{R^2} d\xi' \tag{B4}$$

and its partial derivatives

$$\frac{\partial I_1}{\partial \xi} = -2 \int_{-1}^{1} \frac{(1-\xi'^2)^{1/2}(\xi-\xi')}{R^4} d\xi' \tag{B5}$$

and

$$\frac{\partial I_1}{\partial \zeta} = -2 \int_{-1}^{1} \frac{(1-\xi'^2)^{1/2}\zeta}{R^4} d\xi' \tag{B6}$$

The result may be written

$$\begin{pmatrix} \tilde{\sigma}_x \\[3mm] \tilde{\tau}_{xz} \\[3mm] \tilde{\sigma}_z \end{pmatrix} = \frac{\zeta^2}{\pi} \begin{pmatrix} -\partial I_1/\partial \zeta - 2I_1/\zeta \\[3mm] \partial I_1/\partial \xi \\[3mm] \partial I_1/\partial \zeta \end{pmatrix} \tag{B7}$$

To evaluate I_1 we note it may be cast in the form

$$I_1(\xi,\zeta) = \mathrm{Im}\left[-\frac{1}{\zeta} \int_{-1}^{1} \frac{(1-\xi'^2)^{1/2}}{z-\xi'} d\xi' \right] \tag{B8}$$

where z is the complex variable $\xi + i\zeta$. Written in this way, the integral in equation (B8) is now of standard form and may be expressed as

$$I_2(z) = \int_{-1}^{1} \frac{(1-\xi'^2)^{1/2}}{z-\xi'} d\xi' = \pi\left[z - (z^2-1)^{1/2} \right] \tag{B9}$$

Note that $I_2(z)$ is analytic everywhere except when $|z| = 1$ at the edges of the contact region on the bounding surface, so that it is actually the z-derivative of

$$I_3(z) = \int_{-1}^{1} (1-\xi'^2)^{1/2} \ln(z-\xi') d\xi' \tag{B10}$$

In turn, I_3 is closely related to the integral in equation (38) which essentially is the limit of I_3 as $\zeta \to 0$. Thus it is possible to derive all the present two-dimensional results

from $I_3(z)$ as in reference 9, although it proves algebraically simpler to begin with $I_1(z)$.

To obtain I_1 we first extract the imaginary part of $(z^2-1)^{1/2}$, denoted by β. The actual expression for β may be written

$$\beta = \left[\alpha^2 - (\xi^2 - \zeta^2 - 1)\right]^{1/2}\Big/\sqrt{2} \qquad \text{(B11)}$$

with α given by

$$\alpha^4 = (\xi^2 - \zeta^2 - 1)^2 + 4\xi^2\zeta^2 \qquad \text{(B12)}$$

In terms of the auxiliary variable β we have

$$I_1 = \pi(\beta/\zeta - 1) \qquad \text{(B13)}$$

leading to

$$
\left.
\begin{aligned}
\tilde{\sigma}_x &= 2\zeta - \beta - \zeta\frac{\partial\beta}{\partial\zeta}\\[1em]
\tilde{\tau}_{xz} &= \zeta\frac{\partial\beta}{\partial\xi}\\[1em]
\tilde{\sigma}_z &= -\beta + \zeta\frac{\partial\beta}{\partial\zeta}
\end{aligned}
\right\} \qquad \text{(B14)}
$$

More explicitly in terms of α and β, equations (B14) may be written

$$
\left.
\begin{aligned}
\tilde{\sigma}_x &= 2\zeta - \beta - (\xi^2 + \zeta^2 + 1 + \alpha^2)(\zeta^2/2\beta\alpha^2)\\[0.8em]
\tilde{\tau}_{xz} &= (\xi^2 + \zeta^2 - 1 - \alpha^2)(\zeta\xi/2\beta\alpha^2)\\[0.8em]
\tilde{\sigma}_z &= -\beta + (\xi^2 + \zeta^2 + 1 + \alpha^2)(\zeta^2/2\beta\alpha^2)
\end{aligned}
\right\} \qquad \text{(B15)}
$$

In figures 6 to 8 these stress components have been plotted on planes at various depths ζ beneath the contact plane as functions of the transverse coordinate ξ.
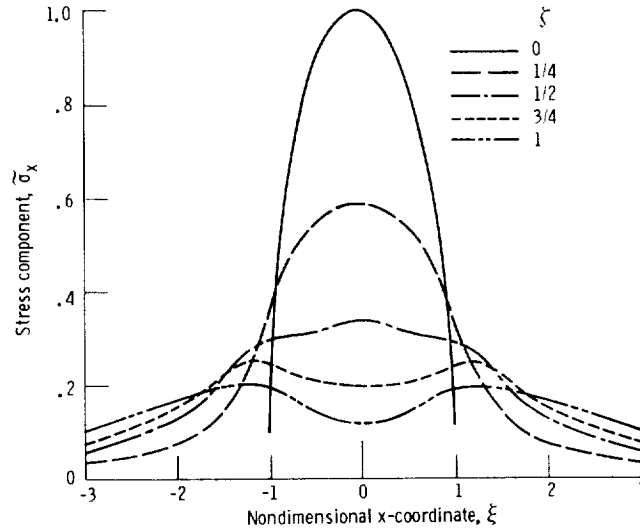

Figure 6.—Curves of stress component $\tilde{\sigma}_x$ perpendicular to load q applied along normal to surface $\zeta = 0$.
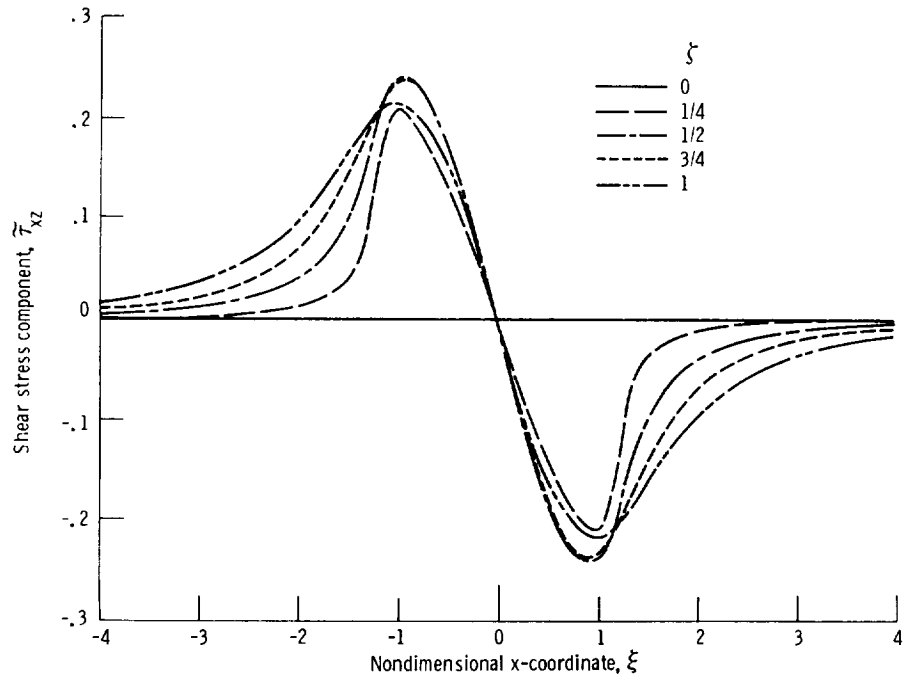
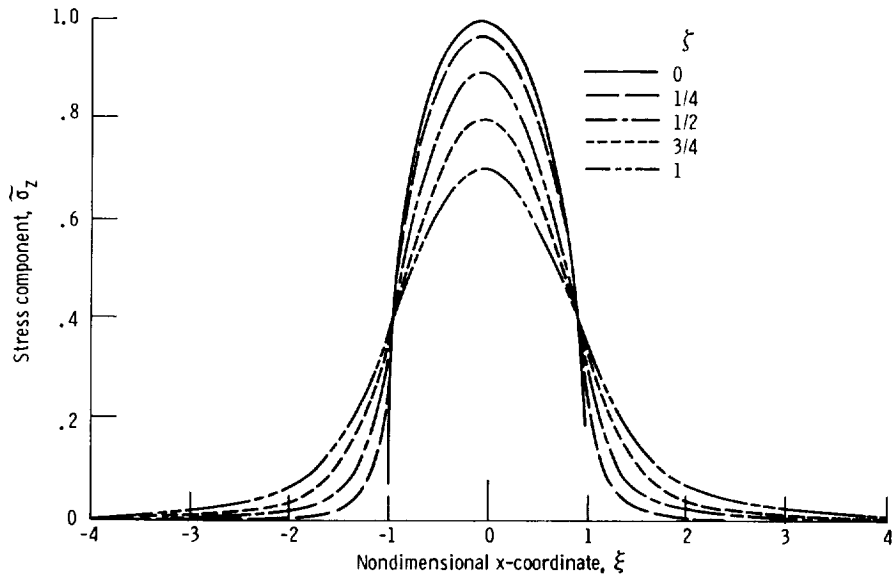Figure 7.—Curves of shear stress component $\tilde{\tau}_{xz}$ for load q normal to surface $\zeta = 0$.

Figure 8.—Curves of stress component $\tilde{\sigma}_z$ along direction of load q normal to surface $\zeta = 0$.

Appendix C
Two Opposed Line Forces Acting on a Circular Cylinder

The stress tensor for the problem of two diametrically opposed concentrated line forces acting on a circular cylinder is derived readily from that of equation (32) for a single line force on a plane boundary by observing that the surfaces of constant radial stress in that case are circular cylinders tangent to the half-space at the origin with diameter $D = R/\cos \psi$. The corresponding radial stress value is $-2q/\pi D$. Superimpose on this the stress arising from an opposed line force q_1 acting at the opposite end of some diameter D (see fig. 9). Since $\psi + \psi_1 = \pi/2$ for any point M on this cylindrical surface, then for such points only the (R,ψ) directions for q coincide with the (ψ_1, R_1) directions, respectively, for q_1. Thus, if $q = q_1$, the state of stress at M in the x,z-plane becomes an isotropic pressure $(-2q/D)$. Finally, reduce this pressure to zero by superimposing everywhere an isotropic tension of the same magnitude. The cylindrical surface is now stress free except along the lines of action of the two forces themselves. The cylinder may thus be mechanically isolated from the elastic half-space, and the resulting stress tensor becomes the required solution for a cylinder of the particular diameter D. For the general interior point with coordinates (R,ψ) or (R_1,ψ_1), the stress components referred to fixed (x,y,z) directions have the plane strain values
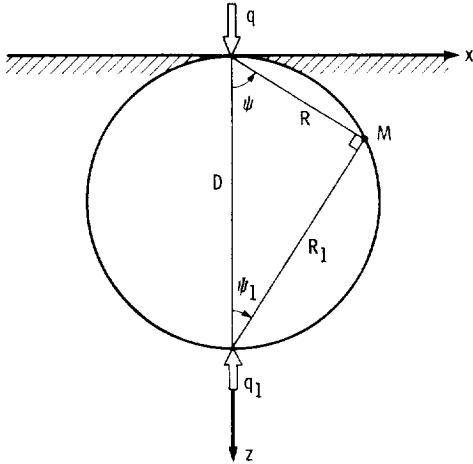

Figure 9.—In x,z-plane two concentrated forces act along normal to bounding surface of elastic half-space, shown shaded. Force q acts at surface along $+z$-axis while force q_1 acts at depth D in opposite direction. M is any point on circle constructed with segment D of z-axis as diameter, having polar coordinates (R,ψ) and (R_1,ψ_1) relative to points of action of two forces.

$$\sigma_x = \frac{2q}{\pi} \left(\frac{1}{D} - \frac{\cos \psi \sin^2 \psi}{R} - \frac{\cos \psi_1 \sin^2 \psi_1}{R_1} \right)$$

$$\sigma_y = \nu(\sigma_x + \sigma_z) = \frac{2\nu q}{\pi} \left(\frac{2}{D} - \frac{\cos \psi}{R} - \frac{\cos \psi_1}{R_1} \right)$$

$$\sigma_z = \frac{2q}{\pi} \left(\frac{1}{D} - \frac{\cos^3 \psi}{R} - \frac{\cos^3 \psi_1}{R_1} \right) \tag{C1}$$

$$\tau_{xz} = -\frac{2q}{\pi} \left(\frac{\cos^2 \psi \sin \psi}{R} - \frac{\cos^2 \psi_1 \sin \psi_1}{R_1} \right)$$

$$\tau_{yz} = \tau_{xy} = 0$$

Corresponding Cartesian displacement components are given by

$$u = -\frac{q}{\pi E'} \frac{1 - 2\nu}{1 - \nu} \left[(\psi + \psi_1) - \frac{1}{2(1 - 2\nu)} \right.$$

$$\left. \times (\sin 2\psi + \sin 2\psi_1) - \frac{1}{D}(R \sin \psi + R_1 \sin \psi_1) \right]$$

$$v = 0 \tag{C2}$$

$$w = -\frac{q}{\pi E'} \left[2 \ln \frac{R}{R_1} + \frac{1}{1 - \nu}(\sin^2 \psi - \sin^2 \psi_1) \right.$$

$$\left. - \frac{1 - 2\nu}{1 - \nu} \frac{1}{D}(R \cos \psi - R_1 \cos \psi_1) \right]$$

$$- \frac{q}{\pi E'} \left(2 \ln \frac{D - d_0}{d_0} - \frac{1 - 2\nu}{1 - \nu} \frac{D - 2d_0}{D} \right)$$

In this representation, the datum point still lies on the z-axis at distance d_0 from the application point of the first force q. Since the shortening $\delta l(x)$ of a chord parallel to the z-axis at distance x is just the difference between w values at its ends, it is clear from the separability of terms in d_0 shown in equation (C2) that δl is now quite independent of reference point. When $x << D$, approximate values for $(R,\psi; R_1,\psi_1)$ are $(x, \pi/2; D,0)$ at the upper end and $(D,0; x,\pi/2)$ at the lower end of the chord. The shortening is found to be

$$\delta l(x) = \frac{4q}{\pi E'} \left(\ln \frac{D}{x} - 1 \right) \tag{C3}$$

by substituting in equation (C2) for w.

The logarithmic singularity in equation (C3) is easily handled in the usual way by distributing the concentrated line force across a small but finite width. A distribution of the type in equation (49) then leads to the compliance result of equation (50). In particular for $\beta = 1/2$, the contact matching condition is met for compression of the cylinder between parallel flats, provided the contact semiwidth is obtained from equation (41). The compliance is then given by equation (47).

References

1. Johnson, K.L.: One Hundred Years of Hertz Contact. Proc. Inst. Mech. Eng., vol. 196, Dec. 1982, pp. 363-378.
2. Timoshenko, S.P.; and Goodier, J.N.: Theory of Elasticity. Second ed. McGraw-Hill, 1951.
3. Goodman, L.E.: Contact Stress Analysis of Normally Loaded Rough Spheres. J. Appl. Mech., vol. 29, no. 3, Sept. 1962, pp. 515-522.
4. Hamrock, B.J.; and Brewe, D.E.: Simplified Solution for Stresses and Deformation. J. Lubr. Technol., vol. 105, no. 2, Apr. 1983, pp. 171-177.
5. Huber, M.T.: Zur Theorie der Berührung fester elastische Körper. (Contract of Solid Elastic Bodies). Ann. Phys., (Leipzig), vol. 14, no. 1, May 1904, pp. 153-163.
6. Belajef, N.M.: Bull. Inst. Engrs. Ways Communications (St. Petersburg, Russia), 1917.
7. Thomas, H.R.; and Hoersch, V.A.: Stresses Due to the Pressure of One Elastic Solid upon Another. Bull.—Ill., Univ., Eng. Exp. Stn., vol. 27, no. 4b, July 15, 1930.
8. Huber, M.T.; and Fuchs, S.: Spannungsverleitung bei der Berührung zweier elastische Zylinder. Phys. Zeitschr., vol. 15, 1914, pp. 298.
9. Poritsky, H.: Stresses and Deflections of Cylindrical Bodies in Contact with Application to Contact of Gears and of Locomotive Wheels. J. Appl. Mech., vol. 17, 1950, pp. 191-201.
10. Smith, J.O.; and Liu, G.K.: Stresses due to Tangential and Normal Loads on an Elastic Solid with Application to Some Contact Stress Problems. J. Appl. Mech., vol. 20, no. 2, June 1953, pp. 157-166.
11. Kalker, J.J.: Surface Displacement of an Elastic Half-Space in a Slender, Bounded, Curved Surface Region with Application to Calculation of Contact Pressue Under a Roller. J. Inst. Math. Its Appl., vol. 19, no. 2, 1977, pp. 127.
12. Muskhelishvili, N.I., (J.R.M. Radok, transl.): Some Basic Problems in the Mathematical Theory of Elasticity. P. Noordhoof Ltd., Groningen, Holland, 1953.
13. Loo, T.-T.: Effect of Curvature on the Hertz Theory for Two Circular Cylinders in Contact. J. Appl. Mech., vol. 25, no. 1, Mar. 1958, pp. 122-124.
14. McCallion, H.; and Truong, N.: The Deformation of Rough Cylinders Compressed Between Smooth Flat Surfaces of Hard Blocks. Wear, vol. 79, no. 3, July 15, 1982, pp. 347-361.
15. Nikpur, K.; and Gohar, R.: Deflexion of a Roller Compressed Between Platens. Tribol. Int., vol. 8, no. 1, Feb. 1975, pp. 2-8.
16. Greenwood, J.A.; and Tripp, J.H.: The Elastic Contact of Rough Spheres. J. Appl. Mech., vol. 34, no. 1, Mar. 1967, pp. 153-159.

TABLE I—THREE-DIMENSIONAL STRAIN

[Rigid bodies are shown shaded. When one body only is elastic, its elastic modulus is E', while subscripts are used to distinguish bodies of different modulus. A similar convention applies to radii of curvature. Negative values denote the radius of a surface concave as viewed from outside the material.]

(a) One body elastic

Rigid ellipsoid on elastic half-space[a]		
	General ellipsoid, semiaxes A_0, B_0, C_0	Sphere, radius R_0
	$R_x = A_0^2/C_0,\ R_y = B_0^2/C_0$	$R_x = R_y = R_0$
	$1/R = 1/R_x + 1/R_y$	$1/R = 2/R_0$
	$\alpha = R_y/R_x\quad \alpha \ge 1$	$\alpha = 1$
	$\Gamma = \left(\dfrac{1}{R_x} - \dfrac{1}{R_y}\right)R\quad \Gamma \ge 0$	$\Gamma = 0$
	$\kappa = b/a = \left(1 - \epsilon^2\right)^{1/2}$	$\kappa = 1,\ \epsilon = 0$
	$\kappa = \left(\dfrac{\alpha D}{B}\right)^{1/2} = \left[\dfrac{2K - (1+\Gamma)\mathcal{E}}{(1-\Gamma)\mathcal{E}}\right]^{1/2}$	-------------
	$a = \left(3FR\mathcal{E}/\pi E'\kappa\right)^{1/3}$	$a = \left(3FR_0/4E'\right)^{1/3}$
	$b = \kappa a$	$b = a$
	$d = \left(K/\mathcal{E}\right)\left(a^2/2R\right)$	$d = \left(a^2/R_0\right)$
	$p = p_0\left(1 - \dfrac{x^2}{a^2} - \dfrac{y^2}{b^2}\right)^{1/2}$	$p = p_0\left(1 - \dfrac{x^2 + y^2}{a^2}\right)^{1/2}$
	$p = \dfrac{F}{\pi ab} = \dfrac{2}{3}p_0$	$p = \dfrac{F}{\pi a^2} = \dfrac{2}{3}p_0$
	$p_0 = \dfrac{1}{2\mathcal{E}}\dfrac{E'a}{R} = \left(\dfrac{3E'^2}{8\pi\mathcal{E}^2R^2\kappa}F\right)^{1/3}$	$p_0 = \dfrac{1}{\pi}\dfrac{2E'a}{R_0} = \dfrac{1}{\pi}\left(\dfrac{6E'^2}{R_0^2}F\right)^{1/3}$

Rigid flat on elastic ellipsoid or sphere	
	All results for the rigid ellipsoid on elastic half-space apply. d is the approach of the center of the elastic body toward the flat.
	Corollary: The diametral shortening of an ellipsoid or sphere compressed between two parallel rigid flats is $2d$.

[a] The argument of the complete elliptic integrals B, D, E, and K is ϵ in every instance.

21

TABLE I.—Concluded.

(b) Two bodies elastic

Two elastic ellipsoids with aligned principal axes	
	$$\frac{1}{R_x} = \left(\frac{1}{R_x}\right)_1 + \left(\frac{1}{R_x}\right)_2$$ $$\frac{1}{R_y} = \left(\frac{1}{R_y}\right)_1 + \left(\frac{1}{R_y}\right)_2$$ $$\frac{1}{E'} = \frac{1}{E'_1} + \frac{1}{E'_2}$$ In terms of these composite variables all formulae of table I(a) apply. $d = d_1 + d_2$ is the approach of centers, where $d_i = [E'/E'_i]d$ is the compliance of body i for $i = 1,2$.
	Corollary 1: For contact between elastic ellipsoid (1) and flat (2), take the limit as the radii of body 2 become infinite. d is the approach of center of ellipsoid 1 toward undeformed surface of flat, d_1 is the compression of the ellipsoid itself; and d_2 is the indentation depth of the flat.
	Corollary 2: For compression of ellipsoid between two dissimilar ellipsoids or flats, appropriate upper (u) and lower (l) composite variables are required, yielding individual upper and lower values of quantities a, b, and d. Net diametral compression for the central ellipsoid 1 is $[E'_u d_u + E'_l d_l]E'_1$.
	Corollary 3: For contact of cylinders crossed at right angles, take the limit as $(R_x)_2$ and $(R_y)_1$ become infinite.

TABLE II.—PLANE STRAIN

[Rigid bodies are shown shaded. When one body only is elastic, its elastic modulus is E', while subscripts are used to distinguish bodies of different modulus. A similar convention applies to radii of curvature. Negative values denote the radius of a surface concave as viewed from outside the material.]

(a) One body elastic

Rigid cylinder on elastic half-space	
	$$a = 2\left(\frac{Rq}{\pi E'}\right)^{1/2} \qquad \text{(A)}$$ $$d = \frac{2q}{\pi E'}\left[\ln\frac{2d_0}{a} - \frac{\nu}{2(1-\nu)}\right] \qquad \text{(B)}$$ $$p = p_0\left(1 - \frac{x^2}{a^2}\right)^{1/2}$$ $$p = \frac{q}{2a} = \frac{\pi}{4}p_0$$ $$p_0 = \frac{E'a}{2R} = \left(\frac{E'q}{\pi R}\right)^{1/2}$$

Rigid flat on elastic circular cylinder[a]	
	The contact semiwidth is given by equation (A). The radial shortening or approach of center of elastic body toward the flat becomes $$d = \frac{2q}{\pi E'}\left(\ln\frac{4R}{a} - \frac{1}{2}\right) \qquad \text{(C)}$$
	Corollary: The diametral shortening of a cylinder compressed between two parallel rigid flats is $2d$.

[a]To obtain approximate results for noncircular cylinders, R must be assigned two distinct meanings: to find contact semiwidth a, R is the radius of curvature at the initial contact point; to find compliance d, R is the distance of the geometric center of cylinder from the initial contact point. The accuracy of this approximation for d decreases as these two values for R diverge.

TABLE II.—Concluded.

(b) Two bodies elastic

Two elastic circular cylinders[a,b]	
	$$\frac{1}{R} = \frac{1}{R_1} + \frac{1}{R_2}$$ $$\frac{1}{E'} = \frac{1}{E_1'} + \frac{1}{E_2'}$$ In terms of these composite variables the contact semiwidth is given by equation (A). The compliances d_i follow from equation (C) using individual values for E' and R. Thus, net compliance or approach of centers is $$d = d_1 + d_2 = \frac{2q}{\pi}\left[\frac{1}{E_1'}\left(\ln\frac{4R_1}{a} - \frac{1}{2}\right) + \frac{1}{E_2'}\left(\ln\frac{4R_2}{a} - \frac{1}{2}\right)\right]$$ $$= \frac{2q}{\pi E'}\left(\ln\frac{4}{a} - \frac{1}{2}\right) + \frac{2q}{\pi}\left(\frac{\ln R_1}{E_1'} + \frac{\ln R_2}{E_2'}\right)$$
	Corollary: For compression of cylinder between two dissimilar cylinders, appropriate upper (u) and lower (l) composite variables are required, yielding individual upper and lower values of quantities a and d. Net diametral compression for the central cylinder 1 is $$d = (d_1)_u + (d_1)_l = \frac{4q}{\pi E_1'}\left(\ln\frac{4R_1}{\sqrt{a_u a_l}} - \frac{1}{2}\right)$$

[a]To obtain approximate results for noncircular cylinders, the same procedure as given in the footnote to table II(a) should be followed.

[b]In limit $R_2 \to \infty$ cylinder 2 becomes a flat. This configuration may be included provided the expression for d_2 is given by equation (B) rather than by equation (C). The infinite result in the latter case is correct but uninformative.

1. Report No.	2. Government Accession No.	3. Recipient's Catalog No.
NASA TP-2473		

4. Title and Subtitle	5. Report Date
Hertzian Contact in Two and Three Dimensions	July 1985
	6. Performing Organization Code
	505-33-62

7. Author(s)	8. Performing Organization Report No.
John H. Tripp	E-2256
	10. Work Unit No.

9. Performing Organization Name and Address	11. Contract or Grant No.
National Aeronautics and Space Administration Lewis Research Center Cleveland, Ohio 44135	
	13. Type of Report and Period Covered
12. Sponsoring Agency Name and Address	Technical Paper
National Aeronautics and Space Administration Washington, D.C. 20546	14. Sponsoring Agency Code

16. Abstract

The basic solution to the problem of mechanical contact between elastically deforming solids was proposed by Hertz over a century ago and has been used by tribologists and others ever since in a steadily increasing number of applications. While the theoretical development is not conceptually difficult and treatments exist to suit all tastes, it is nonetheless interesting to trace the relationships among the solutions in different dimensions. Such an approach is used herein to shed light on the curious and sometimes perplexing behavior of line contacts. A final object of this brief review is simply to gather a number of the more frequently used contact expressions together as a convenient reference and for comparative purposes.

17. Key Words (Suggested by Author(s))	18. Distribution Statement
Surface contact Hertz analysis Elastic compliance Contact stress/strain tensors	Unclassified - unlimited STAR Category 37

19. Security Classif. (of this report)	20. Security Classif. (of this page)	21. No. of pages	22. Price*
Unclassified	Unclassified	24	A02

NASA-Langley, 1985